Sensing light and sound velocities of liquids in two-dimensional phoxonic crystals

Samira Amoudache, Rayisa Moiseyenko, Yan Pennec, Bahram Djafari-Rouhani, Antoine Khater, Ralf Lucklum, Rachid Tigrine

Sensing light and sound velocities with phoxonic crystal

Samira Amoudache[a, b], Rayisa Moiseyenko[a], Yan Pennec[a], Bahram Djafari Rouhani[a], Antoine Khater[c], Ralf Lucklum[d], and Rachid Tigrine[b]

[a] Institut d'Electronique, de Microélectronique et de Nanotechnologie, UMR CNRS 8520, Université Lille 1, 59655 Villeneuve d'Ascq, France
[b] Laboratoire de Physique et Chimie Quantique, Université Mouloud Mammeri, B.P. 17 RP, 15000 Tizi-Ouzou, Algérie
[c] Laboratoire de Physique de l'Etat Condensé, Université du Maine, 72085 Le Mans, France
[d] Institute of Micro and Sensor Systems (IMOS), Otto-von-Guericke-University, Magdeburg, Germany

ABSTRACT

We study theoretically the potentiality of dual phononic-photonic (the so-called phoxonic) crystals for liquid sensing applications. We investigate the existence of well-defined features (peaks or dips) in the transmission spectra of acoustic and optical waves and estimate their sensitivity to the sound and light velocities of the liquid environment. Two different sensors are investigated. In the first one, we study the in-plane transmission through a two-dimensional (2D) crystal made of cylindrical holes in a Si substrate where one row of holes is filled with a liquid. In the second one, the out of plane propagation is investigated when considering the transmission of the incident wave perpendicular to a periodic array of holes in a slab. Such ultra compact structure is shown to be a label-free, affinity-based acoustic and optical nanosensor, useful for biosensing applications in which the amount of analyte can be often limited.

*yan.pennec@univ-lille1.fr

Keywords: Phononic, Photonic Crystal Sensor, Simulations, Confinement, Resonances

1. INTRODUCTION

Photonic crystals [1, 2] and their acoustic counterpart, the so-called phononic crystals [3] are now well-known for their ability to guide, control, and manipulate the propagation of the optic and acoustic waves. These properties are mainly related to the possibility of band gaps in their band structure that allow the existence of localized modes and confined optic/acoustic waves. Moreover, during the past few years, there has been an increasing interest towards structures exhibiting simultaneous phononic and photonic band gaps, the so-called phoxonic crystals, thus allowing dual confinement of phonons and photons [4, 5]. From the point of view of sensing applications, several papers have already shown the capability of photonic crystals for detecting small variations in the refractive index of gases and liquids and have opened the way to a platform for a new class of sensors. In general, the sensing phenomena is based on the high sensitivity of localized modes (associated with defects) appearing inside the gaps of the photonic crystals to the variation of the index of refraction in the surrounding fluid [6-8]. In a recent work [9], some authors have also studied the normal transmission through a slab perforated periodically with holes and measured the shift of a well-defined feature in the spectrum with the refractive index of the embedding liquid. In contrast, phononic crystals have only been recently proposed as a possible platform for the investigation of the acoustic velocity of a liquid filling the hollow parts of the structure [10, 11]. Thus, the potentiality of different geometries of phononic crystals for sensing applications still needs several further investigations. Moreover, some of the structures may be suitable for a dual measurement of both acoustic and optical velocities of the analyte. The general background is the great deal of works we have devoted during the last few years to the engineering of the dispersion curves and band gaps in phononic [3] and phoxonic [4, 12] crystal slabs.

To make a phononic/photonic sensor, one needs to design a structure in which the transmission coefficient displays well-defined features that are very sensitive to the acoustic/optic velocity of the infiltrating liquid. These features should be relatively isolated in frequency in order to allow the sensing of the probed parameter on a sufficiently broad range. In

this paper, we investigate theoretically the transmission spectra in two geometries of periodic crystals and discuss the physical origin of the peaks and dips in the spectra and their usefulness for the sensing applications.

Two configurations are considered for the propagation of the incident waves with respect to the phoxonic crystal. In the case of in-plane propagation, we study the transmission coefficient through a two-dimensional (2D) crystal made of cylindrical holes in a silicon substrate where one row of holes is filled with a liquid. In the case of out-of plane configuration, we study the transmission of the incident wave normally to a slab perforated periodically with holes.

The FDTD approach has been used to resolve the photonic and phononic wave propagation. This method solves either the electromagnetic or the elastic wave equations by discretizing time and space and by replacing derivatives by finite differences in the equations of motion. As compared to other numerical method such as plane wave expansion (PWE), it presents the advantage of allowing simulation of mixed phononic structures, composed of both fluids and solids. The results for the two incident configurations are respectively presented in sections 2 and 3. Some conclusions are drawn in section 4.

2. IN-PLANE PROPAGATION

Figure 1a represents a three dimensional (3D) schematic view of the investigated periodic structure composed of a silicon substrate, drilled with infinite air cylinders arranged in a square array of lattice parameter a. Figure 1b represents the elementary unit cell used for the calculation. As seen in figure 1(a), all cylinders of radius r_1 are filled with air except one row of different radius r_2 in the middle of the structure which contains the fluid to be probed. In all the following calculations, the normalized radius of the inclusions constituting the perfect structure is fixed to $r_1/a = 0.25$ while r_2/a is chosen variable for the optimization of the sensor.

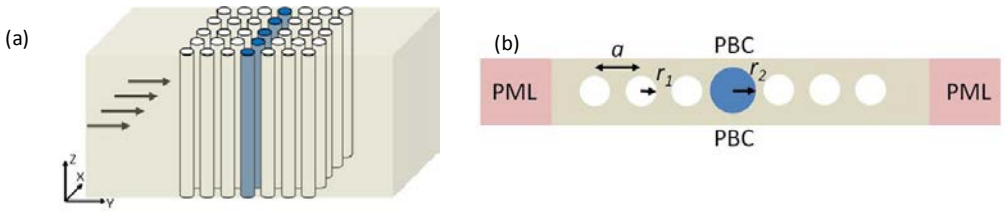

Figure 1: (a) 3D-schematic representation of the phoxonic crystal containing one row of liquid filled cylinders. (b) Elementary unit cell used for the calculation of the transmission of optical and acoustic waves. On each y-boundaries of the unit cell perfect matching layers (PML) are applied while on the x-boundaries periodic boundary conditions (PBC) insure the periodicity of the crystal. The defect line of holes have a radius r_2 which can be different from the radius r_1 of the phoxonic crystal of lattice parameter a.

To study the acoustic waves silicon is considered as a cubic material with the elastic constants $C_{11} = 16.57\ 10^{10}$ N/m^2, $C_{44} = 7.962\ 10^{10}$ N/m^2, $C_{12} = 6.39\ 10^{10}$ N/m^2, and with a mass density $\rho = 2331$ kg/m^3. The acoustic wave velocity in water has been taken equal to $c_{liq} = 1490$ m/s. From the optical point of view silicon behaves as an isotropic medium with a refractive index n = 3.5. The surrounding air is considered as a vacuum with a refractive index n = 1 and the refractive index for the water is 1.33. The transmission curves are presented as a function of a normalized frequency $\Omega = \omega a/2\pi c$, where ω is the angular frequency (in s^{-1}), and c is either the velocity of light in vacuum for the electromagnetic waves or the transverse velocity of sound in the direction [001] in silicon for the elastic waves.

Phononic crystals

In phononic, figure 2(a) represents the transmission coefficient through the water filled structure (black solid lines) together with the transmission through the perfect crystal (red dashed lines) for comparison. The introduction of the water holes leads to new well-defined features at the following reduced frequencies $\Omega_A = 0.301$, $\Omega_B = 0.482$, and $\Omega_C = 0.627$ which appear either as peaks or dips in the transmission coefficient depending on whether they fall in the band gap or in the pass band of the perfect crystal.

The calculations of the displacement field at these specific frequencies are reported figure 2(b). One can see clearly that the elastic field is strongly localized inside the water hole meaning that the peaks and dips A, B, and C correspond to eigenmodes of the water hole in interaction with the incident wave. Due to the large contrast between the acoustic velocities and impedances of water and Si, these modes can be considered as cavity resonances inside the holes

surrounded by an almost rigid material and, therefore, their frequencies are very close to the solution of the equation $J'_m(\omega r_2 / c_{liq}) = 0$ where J'_m is the derivative of the Bessel function of order m.

The frequencies of the defect modes can be tuned by varying the radius of the water hole. As seen in figure 2(c), when r_2/a increases, the frequencies of the defect modes decrease and become closer to each other. Therefore, for the purpose of sensing acoustic velocities, it would be more suitable to do not increase too much the radius of the defect cylinders inside the phononic crystal.

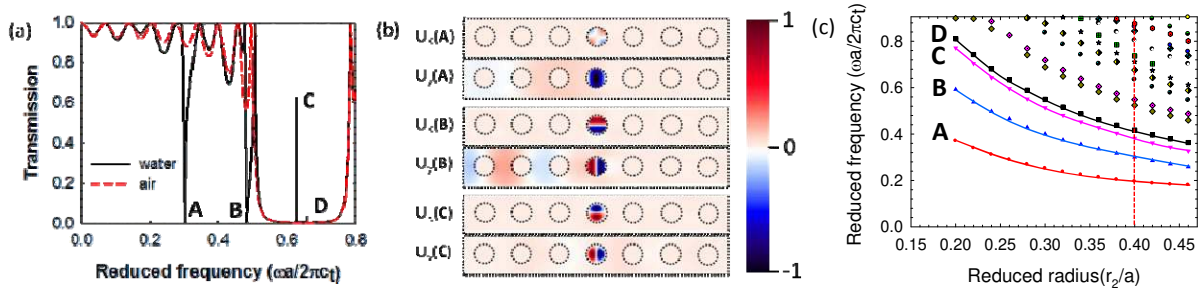

Figure 2: (a) Transmission curve when the radius of the centered cylinder is $r_2/a=0.25$ and filled with water (solid black line). The red dashed curve corresponds to the transmission through a perfect crystal. (b) Maps of the displacement field at the dips A, B and C. (c) Evolution of the frequencies as a function of the radius of the water hole, r_2/a.

Photonic crystals

In photonic we have considered the transverse electric (TE) polarization of the electromagnetic field, i.e. when the electric field is parallel to the plane of periodicity of the crystal (O, x, y). We first calculate the photonic transmission through the structure of figure 1, where the central hole of radius $r_1/a = r_2/a = 0.25$ is filled with water. Unfortunately, the introduction of such a defect does not give rise to any peak in the forbidden photonic band gaps. It then appears necessary to change the radius of the defect hole. Figures 3(a) show the (TE) transmission magnified in the reduced frequency range [0.385, 0.435] and through the 2D photonic crystal when the radius of the water hole is taken to be $r_2/a = 0.4$. The transmission spectrum now presents new peaks inside the band gap. The peak (α) at the reduced frequency 0.402 appears with a good quality factor and almost isolated in the middle of the band gap.

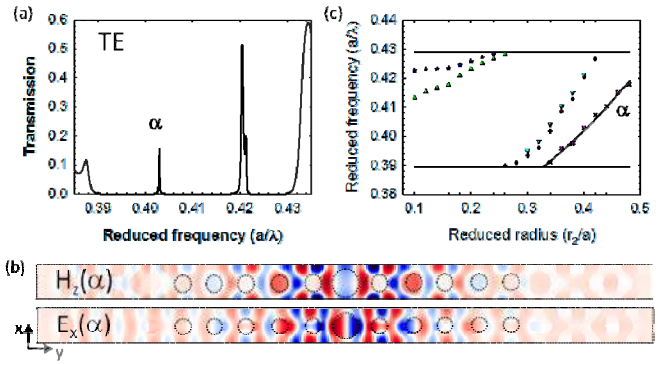

Figure 3: (a) Photonic transmission for TE polarizations through the photonic crystal for the radius $r_2/a = 0.4$ of the water hole. (b) Map of the electromagnetic fields for the frequencies of the mode α. (c) Evolution of the resonant frequencies inside the photonic band gap as a function of the radius r_2/a for TE polarization.

The map of its electromagnetic field is presented figure 3(b). In contrast to the phononic modes, the electromagnetic field is not only confined in the water hole but extend in the vicinity of the defect. The evolution of the frequency of (α) peak has been investigated as a function of the radius of the water hole and is presented figure 3(c). One can see the existence of four modes which frequencies increase with the radius of the water hole in good agreement with the decrease of the effective refractive index. Among all these modes only the mode α is well isolated from the others and cover the whole band gap width when varying the radius r_2. An equivalent analysis has been performed with the transverse magnetic

(TM) polarization of the electromagnetic field, i.e. when the magnetic field is parallel to the plane of periodicity of the crystal (O, x, y), and show the existence of a high quality peak β due to the water hole defect through the (TM) band gap.

PhoXonic crystal sensor

To make a phoXonic sensor, one needs to design a phononic/photonic structure in which the transmission coefficient displays well-defined features that are very sensitive to the acoustic/optic velocity of the infiltrating liquid. A preliminary condition is that these features should be relatively isolated in order to allow the sensing of the probed parameter on a sufficiently broad range of frequencies. In phononic, figure 2(c) shows that the first two modes A and B satisfy these requirements whatever the radius of the water hole, even though a small radius of the water hole is more favorable. In photonic, as seen in figure 3(c), the radius should be either lower than $r_2/a = 0.2$ or higher than $r_2/a = 0.35$. We will make the demonstration of the dual phononic and photonic sensor dealing with the (α) mode and the radius $r_2/a = 0.4$.

The efficiency of the phoXonic sensor has been tested by changing the physical parameters of the liquid filling the central hole. We have considered a set of mixtures of water and 1-propanol at different molar ratio x, for which the density and speed of sound are different, as well as the refractive index, as reported in table 1.

Table 1: Density ρ_{liq}, speed of sound c_{liq} [10] and refractive index n_{liq} [13] of 1-propanol in water for different molar ratio x.

Molar ratio, x	Density ρ_{liq} (kg/m^3)	Longitudinal sound velocity (c_{liq}) (m/s)	Refractive index (n_{liq})
0 (water)	998	1490	1.333
0.021	990	1545	/
0.054	/	/	1.3476
0.056	974	1588	/
0.2167	/	/	1.3680
0.230	908	1421	/
0.347	881	1367	/
0.596	841	1298	/
0.6873	/	/	1.3835

Figure 4(a) and (b) give respectively the evolution of the phononic and photonic (TE) transmission as a function of the liquid filling the central hole ($r_2/a = 0.4$). The transmitted curves are presented in the relevant ranges of frequency which correspond to the presence of the dips A and B in phononic and the peak α in photonic. For both elastic and optical waves, all features associated to the defect modes present a shift in frequency by changing the nature of the liquid. In phononic, the reduced frequencies of the dips A and B increase as soon as the longitudinal velocity of the liquid increases. In photonic, the frequency of the peak α decreases as a function of the refractive index. It means that if we refer to the velocity of sound and light, an increase of the acoustic (optical) velocity leads to a blue shift of the eigenfrequency of the defect.

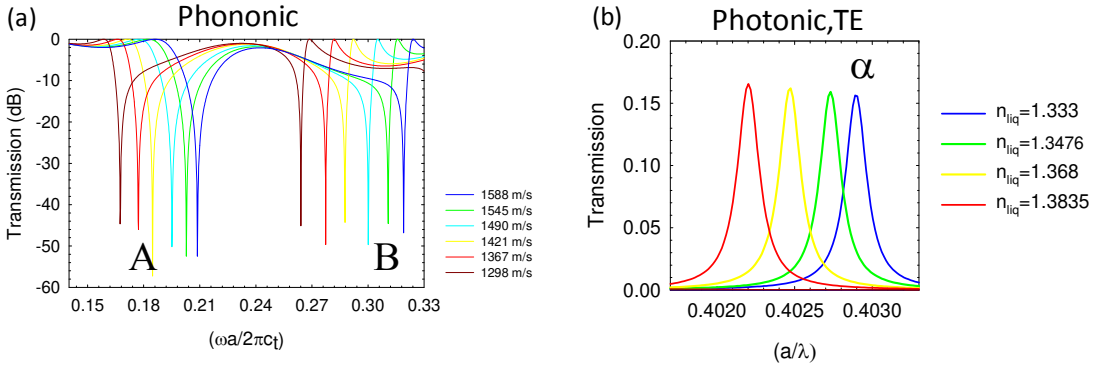

Figure 4: (a) Evolution of the phononic transmission curve (in dB) as a function of the acoustic velocity of the liquid filling the central hole of figure 1(a) for the two modes A and B. (b) Evolution of the photonic (TE) transmission curve as a function of the solvent filling the central hole for the (α) mode.

The most common way to estimate the efficiency of a sensor is to calculate the sensitivity (S) and the figure of merit (FOM) given, in photonic, by the following expressions:

$$S^{j}_{photonic} = \frac{\Delta\lambda_j}{\Delta n_{liq}} \text{ (nm/RIU)}$$

$$FOM^{j}_{photonic} = \frac{S_j \times Q_j}{\lambda_j} \text{ (RIU}^{-1}\text{)}$$

where RIU is the Refractive Index Unit, and Q_j is the photonic quality factor of mode j. In phononic the following comparative expressions can be defined:

$$S^{i}_{phononic} = \frac{\Delta f_i}{\Delta c_{liq}} \text{ (MHz/ms}^{-1}\text{)}$$

$$FOM^{i}_{phononic} = \frac{S_i \times Q_i}{f_i} \text{ (m/s)}^{-1}$$

where Q_i is the phononic quality factor of mode i.

If we choose to work in the telecommunication range (1550nm), the period of the crystal should be taken equal to 640 nm. With this lattice parameter, and when the central hole is filled with water, the wavelength of modes α occurs at 1590 nm while the frequencies of modes A and B are at 1.78 GHz and 2.74 GHz. Table 2 reports the numerical values of the quality factors, sensitivities and figures of merit for the acoustic and optical modes ((TE) and (TM)) when considering a large (r_2 = 0.4a = 256 nm) and a small (r_2 = 0.11a = 70 nm) radius of the water filled central hole. The higher sensitivity and figure of merit in phononic are obtained for the smaller radius while in photonic the larger radius leads to the higher sensitivity and figure of merit.

Table 2: Phononic and photonic sensitivities (S) and figures of merit (FOM)

r_2/a (a=640nm)	S_A	$FOM^{A}_{phononic}$ (m/s)$^{-1}$	S_B	$FOM^{B}_{phononic}$ (m/s)$^{-1}$	S^{TE}	$FOM^{TE}_{photonic}$ (RIU^{-1})	S^{TM}	$FOM^{TM}_{photonic}$ (RIU^{-1})
0.40	1.32	0.14	1.73	0.27	58	150	18	175
0.11	3.60	2.25	/	/	14	40	6	110

3. OUT-OF-PLANE PROPAGATION

Figure 5 represents the 3D schematic view and the elementary unit cell of the investigated structure constituted by a periodically perforated silicon plate arranged in a square array of lattice parameter a in which we consider the excitation of an incident wave normally to the plate. This problem meets the recent interest in the literature about the extraordinary transmission and shielding through sub-wavelength apertures [14-17]. All cylinders present a radius r/a = 0.15 and a thickness of the plate of h/a = 0.25. The plate is embedded in the fluid we want to probe both with acoustic and optical waves.

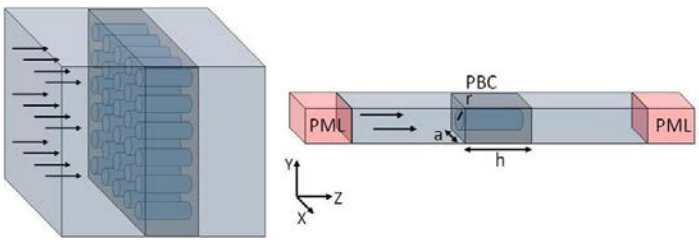

Figure 5: Schematic representation of a normal transmission through a periodically plate embedded in a liquid and the corresponding elementary unit cell used for the calculation. The geometrical parameters are fixed to h/a = 0.25 and r/a = 0.15.

Phononic transmission

Figure 6(a) represents the acoustic transmission coefficient through the plate when the surrounding medium is filled with water. The transmission curve leads to a well defined peak and dip labeled (A) in figure 6(a). The calculation of the displacement field at the frequency of the dip is represented figure 6(b). An analysis of the component u_Y and u_Z of the displacement field shows that the mode is strongly localized at the circular edge of the water cylinder (see $u_Y(y, z)$ and $u_Z(y, z)$) with an evanescent decreases outside (see $u_Y(x, y)$) and inside the water cylinder (see $u_Z(x, y)$). A schematic representation of the motion of the water cylinder is represented figure 6(c) with regard to the two planes (x, y) and (y, z). The excitation of the eigenmode A leads either to a peak or a dip in the transmission coefficient depending whether the incident wave is in-phase or out-of-phase with the eigenmode oscillation. Therefore, since the peak A followed by a dip is sufficiently well-defined and isolated, it can be seen as a good candidate for the purpose of sensing acoustic velocities.

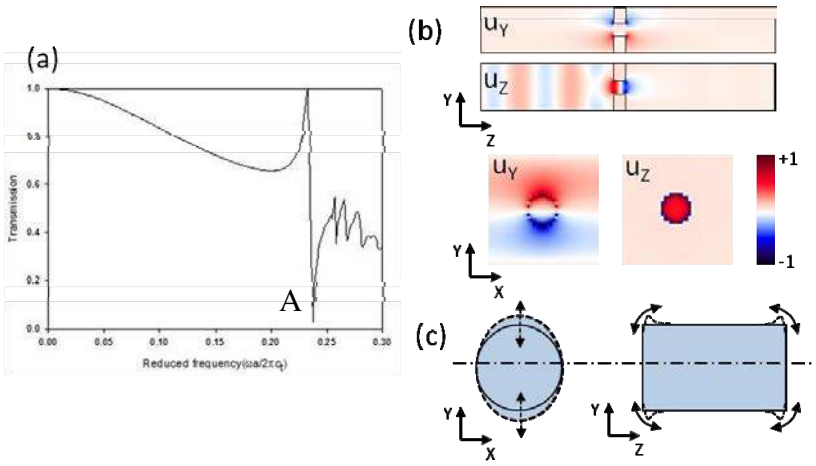

Figure 6: (a) Phononic transmission curve for an incidence normal to the plate when the embedded medium is water with the geometrical parameters h/a = 0.25 and r/a = 0.15. (b) Displacement field calculation at the frequency of the dip A. (c) Schematic representation of mode A with the motion of the circular edges of the water cylinder.

Photonic transmission

In photonic, the calculation of the transmission curve for an incident wave launched perpendicularly to the plate leads also to a well-defined and isolated dip and peak B (figure 7(a)). The map of the electromagnetic field at the frequency of the dip is presented figure 7(b). In contrast with the phononic mode, the electromagnetic field is not only confined inside the water hole but is spread over the whole plate, both inside the water hole and the silicon matrix. One can also notice that the mode is symmetric with respect to the middle plane of the plate. Again, due to its high quality factor and well-isolated frequency, the peak and dip B is suitable for the photonic sensing purpose.

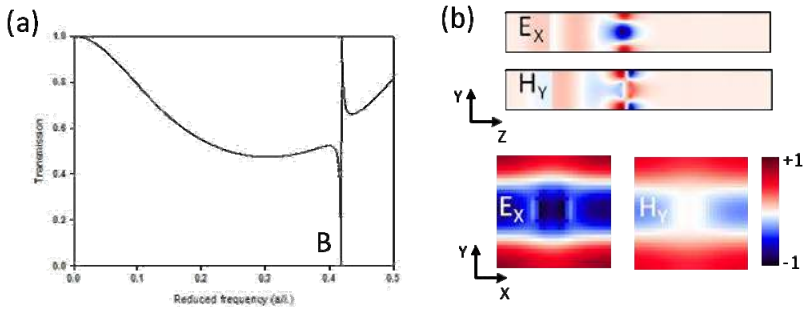

Figure 7: (a) Photonic transmission curve for an incidence normal to the plate when the embedded medium is water with the geometrical parameters h/a = 0.25 and r/a = 0.15a. (b) Map of the electromagnetic field at the frequency of the dip B.

PhoXonic sensor

In this section, we consider the normal transmission through the plate when changing the surrounding fluid medium. We present figure 8(a) and (b) respectively the phononic and photonic transmission spectra for different values of the acoustic velocity and refractive index of refraction of the liquid. For both elastic and optical waves, the two peaks/dips A (phononic) and B (photonic) present a shift in frequency by changing the nature of the liquid. In phononic, the reduced frequency of dip A increases with the longitudinal velocity of the liquid. In photonic, the frequency of dip B decreases as a function of the refractive index. As previously, if we refer to the velocity of sound and light, an increase of the acoustic (optical) velocity leads to a blue shift of the eigenfrequency. If we refer to the same lattice parameter as before (a = 640 nm), the acoustic sensitivity is in the same order of magnitude while in photonic the sensitivity is S = 150nm/RIU, i.e. almost three times higher.

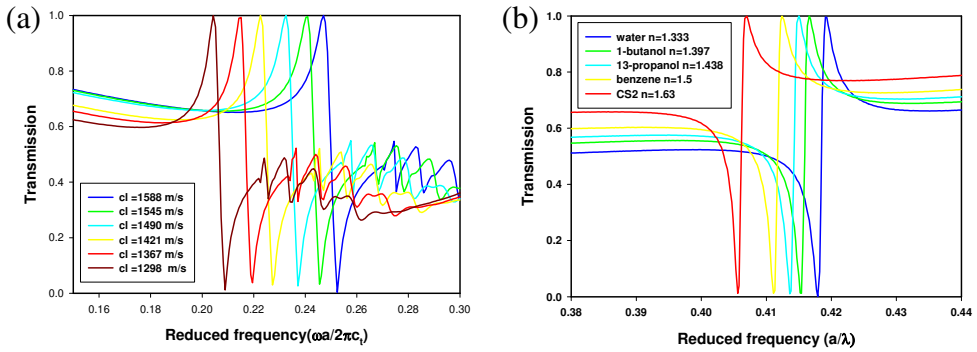

Figure 8. Representation of the phononic (a) and photonic (b) transmission spectra for respectively different acoustic velocity and refractive index of the liquid.

4. CONCLUSIONS

In this work, we investigated the potentiality of an infinite 2D cavity-type phoxonic crystal and a phoxonic plate for sensing the acoustic velocity of a liquid. For sensing applications, the objective has been to design structures in which the phononic/photonic transmission spectra contain well-defined, sufficiently isolated, features, with a high sensitivity to the acoustic/optic parameters of the infiltrating liquid. We studied the first structure for in-plane incident waves and the second when the incoming wave is perpendicular to the phoxonic plate. We identified the physical origin of the specific features appearing in the transmission spectra and discussed the structural parameters useful for making a phoxonic sensor. While the first device is useful for small amount of liquid, in the second one, the plate is totally immersed in the probing fluid, leading to different potential applications.

Acknowledgments: This work was supported by the European Commission Seventh Framework Programs (FP7) under the FET-Open project TAILPHOX N° 233883.

5. REFERENCES

[1] Yablonovitch, E., "Photonic band-gap structures," J. Opt. Soc. Am. B 10, 283 (1993)

[2] Joannopoulos, J. and Winn, J. "Photonic crystal: molding the flow of light, " Princeton Univ. Pr., (2008)

[3] Pennec, Y., Vasseur, J., Djafari-Rouhani, B., Dobrzynski, L., Deymier, P.A., "Two-dimensional phononic crystals: Examples and applications" Surface Science Reports 2010, 65-229 (2010).

[4] Pennec, Y., Djafari-Rouhani, B., El Boudouti, E.H., Li, C., El Hassouani, Y., Vasseur, J.O., Papanikolaou, N., Benchabane, S., Laude, V., Martinez, A., "Simultaneous existence of phononic and photonic band gaps in periodic crystal slabs, " Optics Express 18, 14301 (2010)

[5] Mohammadi, S., Eftekhar, A.A., Khelif, A. and Adibi, A., "Simultaneous two-dimensional phononic and photonic band gaps in opto-mechanical crystal slabs," Optics Express 18, 9164 (2010)

[6] Kurta, H. and Citrin, D. S., "Photonic crystals for biochemical sensing in the terahertz region," Appl. Phys. Lett 87, 041108 (2005)

[7] Wang, X., Xu, Z., Lu, N., Zhu, J., Jin, G., "Ultracompact refractive index sensor based on microcavity in the sandwiched photonic crystal waveguide structure", Optics Communications 281 1725 (2008)

[8] Dündar, M. A., Ryckebosch, Els C. I., Nötzel, R., Karouta, F. L. , IJzendoorn, L. J. and Heijden, R.W., "Sensitivities of InGaAsP photonic crystal membrane nanocavities to hole refractive index," Optics Express 18, 4049 (2010)

[9] Huang, M., Yanik, A. A., Chang, T.-Y. and Altug, H., "Sub-wavelength nanofluidics in photonic crystal sensors," Optics Express 17, 24224 (2009)

[10] Lucklum, R. and Li, "Phononic crystals for liquid sensor applications," J. Meas. Sci. Technol. 20 124014 (2009)

[11] Ke, M., Zubtsov, M. and Lucklum, R., "Sub-wavelength phononic crystal liquid sensor," J. of Appl. Phys. 110, 026101 (2011)

[12] Hassouani, Y. El., Li, C., Pennec, Y., Boudouti, E. H. El., Larabi, H., Akjouj, A., Matar, O. Bou, Laude, V., Papanikolaou, N., Martinez, A. and Djafari Rouhani, B., "Dual phononic and photonic band gaps in a periodic array of pillars deposited on a thin plate," Phys. Rev. B 82, 155405 (2010)

[13] Koohyar, F., Kiani, F., Sharifi, S., Sharifirad, M. and Rahmanpour, S. H., "Study on change on refractive index on mixing, excess molar volume and viscosity deviation for aqueous solution of methanol, ethanol, ethylene glycol, 1-propanol and 1,2,3-propantriol at T = 292.15 K and atmospheric pressure," Res. J. App. Sci. Eng. Technol., 17 3095, (2012)

[14] Hou, B., Mei, J., Ke, M., Wen, W., Liu, Z., Shi, J. and Sheng, P., " Tuning Fabry-Perot resonances via diffraction evanescent waves, " Phys. Rev. B 76, 054303 (2007)

[15] Christensen, J., Martin-Moreno, L. and Garcia-Vidal, F. J., " Theory of resonant acoustic transmission through subwavelength apertures," Phys. Rev. Lett. 101 014301 (2008).

[16] Estrada, H., Garcıa de Abajo, F. J., Candelas, P., Uris, A., Belmar, F. and Meseguer, F., "Angle-dependent ultrasonic transmission through plates with subwavelength hole arrays," Phys. Rev. Lett.102 144301 (2009).

[17] Peng, S., Qiu, C., He, Z., Ye, Y., Xu, S., Tang, K., Ke, M. and Liu, Z. "Extraordinary acoustic shielding by a monolayer of periodical polymethyl methacrylate cylinders immersed in water," Journal of Applied Physics 110, 014509 (2011).